Transition Met Chem (2011) 36:545–551
DOI 10.1007/s11243-011-9501-3

Polyatomic anion versus acetonitrile in coordinating ability: structural properties of AgX-bearing 1,4-bis(2-isonicotinoyloxyethyl)piperazine ($X^- = NO_3^-$, $CF_3SO_3^-$, ClO_4^-, BF_4^-, and PF_6^-)

Chi Won Kim · Jungmin Ahn · Sung Min Kim · Tae Hwan Noh · Ok-Sang Jung

Received: 13 April 2011 / Accepted: 6 May 2011 / Published online: 26 May 2011

Abstract Type studies on competitive polyatomic anion versus acetonitrile coordination in the self-assembly of a series of $[Ag_2(X)_m(bip)(NCCH_3)_n](X)_{2-m}$ ($X^- = NO_3^-$, $CF_3SO_3^-$, ClO_4^-, BF_4^-, and PF_6^-; $m = 0, 2$; $n = 0, 2, 4$; bip = 1,4-bis(2-isonicotinoyloxyethyl)piperazine) were carried out. Each bip spacer acts as an N_4 tetradentate ligand and is linked to four silver(I) centers through two pyridine and two piperazine moieties, producing a double strand consisting of two 20-membered ring units. The coordinating environment around the silver(I) center is subtly determined by the competition of the polyatomic anions with acetonitrile, that is, by the Ag···$NCCH_3$ versus Ag···X interactions. The coordinating ability of acetonitrile is inversely proportional to the order of the coordination ability of the Hoffmeister series of polyatomic anions, $NO_3^- \gg CF_3SO_3^- > ClO_4^- > BF_4^- \gg PF_6^-$.

Introduction

Fascinating diverse coordination skeletons have been designed and constructed via the self-assembly of basic components with varied properties such as metal center geometry, the binding sites of donating atoms and the lengths of spacers, and/or by the induction of weak intra- or intermolecular interactions [1–5]. Research on the rational design of coordination polymers is a fruitful field: polymers have various potential applications in molecular separation, toxic materials adsorption, molecular containers, ion exchangers, molecular recognition, and luminescent sensors [6–10]. In order to effectively construct desirable coordination materials with task-specific motifs, the delicate coordination geometry around the central metal needs first to be considered [11–13]. Anion coordination chemistry is an emerging topic of interest, particularly from environmental pollution, industrial chemical, biological process, ionic liquid, catalysis, lithium battery, and health-related perspectives [14–17]. Recent and promising anion chemistry advances have been made in anion template assembly, ion-pair recognition, and anion functionality [17–20]. Some polyatomic anions in fact play crucial roles in the self-assembly of coordination materials, owing to attributes such as negative charge, a wide range of geometries, significant solvent effects, and pH dependence [21–23]. However, precise control of coordination geometry via (counter)anions remains a rare achievement, due to less effective electrostatic binding interactions. Our previous results on silver(I) complexes revealed a variable skeletal structure, labile anion exchange [4, 5], and a variety of silver(I) coordination geometries [24]. In the present study, for the purposes of elucidating the direct role and coordinating nature of polyatomic anions, the self-assembly of an AgX ($X^- = NO_3^-$, $CF_3SO_3^-$, ClO_4^-, BF_4^-, and PF_6^-) series with 1,4-bis(2-isonicotinoyloxyethyl)piperazine (bip) as a function of the polyatomic anions and temperature was investigated. We discuss, here, the competitive polyatomic anion versus acetonitrile coordination that is the basis of that self-assembly. Nitrate, triflate, perchlorate, tetrafluoroborate, and hexafluorophosphate, ubiquitous in the contexts of chemistry, environmental pollution, disease pathways, and biological processes

Electronic supplementary material The online version of this article (doi:10.1007/s11243-011-9501-3) contains supplementary material, which is available to authorized users.

C. W. Kim · J. Ahn · S. M. Kim · T. H. Noh · O.-S. Jung (✉)
Department of Chemistry, Pusan National University, Pusan 609-735, Korea
e-mail: oksjung@pusan.ac.kr

[25, 26], were selected as anionic balancers for the cationic assembled skeleton.

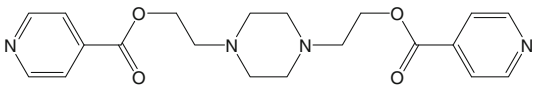

bip

Experimental

Materials and measurements

All of the chemicals were purchased from Aldrich Chemicals and used without further purification. Elemental microanalyses were performed on crystalline samples (C, H, N) by the Pusan Center at KBSI using a Vario-EL III. ^{1}H and ^{13}C NMR spectra were recorded on a Varian Mercury Plus 300 operating at 300 and 75 MHz, respectively, and the chemical shifts were relative to the internal Me_4Si. Infrared spectra were obtained on a Nicolet 380 FTIR spectrophotometer using samples prepared as KBr pellets. The melting points were determined with a Thomas-Hoover capillary melting point apparatus and were not corrected.

Synthesis of 1,4-bis(2-isonicotinoyloxyethyl)piperazine (bip)

Triethylamine (3.48 mL, 25 mmol) was added to a solution of isonicotinoyl chloride hydrochloride (1.958 g, 11 mmol) in chloroform (100 mL) at room temperature. Subsequently, 1,4-bis(2-hydroxyethyl)piperazine (0.871 g, 5 mmol) was added to the reaction solution, which was refluxed for 12 h. The chloroform solution was successively washed with a 0.5 N NaOH solution, after which it was dried using magnesium sulfate and filtered. Evaporation of the solvent produced crystalline 1,4-bis(2-isonicotinoyloxyethyl) piperazine in 82% yield. M.p. 129–131 °C. Anal. Calc for $C_{20}H_{24}N_4O_4$: C 62.5; H 6.3; N 14.6. Found: C 62.5; H 6.3; N 14.6. IR (KBr pellets, cm^{-1}): 2962 (w), 2807 (m), 1720 (s), 1408 (m), 1286 (s), 1128 (m), 964 (m), 752 (m), 703 (m), 678 (m). ^{1}H NMR (300 MHz, $CDCl_3$): δ 8.77 (dd, $J = 1.5$, 4.5 Hz, 4H), 7.82 (dd, $J = 1.5$, 4.5 Hz, 4H), 4.48 (t, $J = 5.7$ Hz, 4H), 2.79 (t, $J = 5.7$ Hz, 4H), 2.62 (s, 8H). ^{13}C NMR (75 MHz, $CDCl_3$): δ 165.13, 150.73, 137.50, 122.94, 63.29, 56.54, 53.42.

Synthesis of $[Ag_2(ClO_4)_2(bip)(CH_3CN)_2]$

$AgClO_4$ (1 mmol, 0.207 g) in water (3 mL) was added to 1,4-bis(2-isonicotinoyloxyethyl)piperazine (bip) (0.5 mmol, 0.192 g) in ethanol (7 mL). The reaction mixture was stirred for 15 min, after which the precipitated powder was filtered off and washed with ethanol several times. The solid was dissolved in acetonitrile and exposed to diethyl ether vapor to yield colorless single crystals suitable for X-ray crystallography in a 70% yield. M.p. 178–182 °C (dec). Anal. Calc for $C_{24}H_{30}N_6O_{12}Cl_2Ag_2$: C 32.7; H 3.4; N 9.5. Found: C 32.7; H 3.4; N 9.5. IR (KBr pellets, cm^{-1}): 2962 (w), 2808 (m), 1720 (s), 1408 (m), 1286 (s), 1090 (s), 966 (w), 754 (m), 704 (m), 625 (m).

Synthesis of $[Ag_2(CF_3SO_3)_2(bip)(CH_3CN)_2]$

A procedure similar to that for $[Ag_2(ClO_4)_2(bip)(CH_3CN)_2]$ was followed. Colorless crystals of $[Ag_2(CF_3SO_3)_2$-$(bip)(CH_3CN)]$ formed in a 75% yield. M.p. 173–177 °C (dec). Anal. Calc for $C_{26}H_{30}Ag_2F_6N_6O_{10}S_2$: C 31.9; H 3.1; N 8.6. Found: C 31.8; H 3.1; N 8.6. IR (KBr pellets, cm^{-1}): 2960 (w), 2808 (w), 1722 (s), 1408 (m), 1286 (s), 1167 (m), 1128 (m), 1034 (m), 964 (m), 754 (m), 704 (m), 644 (m), 521 (s).

Synthesis of $[Ag_2(BF_4)_2(bip)(CH_3CN)_2]$

Colorless crystals of $[Ag_2(BF_4)_2(bip)(CH_3CN)]$ formed in a 75% yield. M.p. 177–181 °C (dec). Anal. Calc for $C_{24}H_{30}B_2N_6O_4F_8Ag_2$: C 33.7; H 3.5; N 9.8. Found: C 33.7; H 3.6; N 9.8. IR (KBr pellets, cm^{-1}): 2962 (w), 2808 (m), 1722 (s), 1410 (m), 1286 (s), 1065 (s), 964 (m), 754 (m), 704 (m), 523 (w).

Synthesis of $[Ag_2(bip)(CH_3CN)_4](PF_6)_2$

Colorless crystals of $[Ag_2(bip)(CH_3CN)_2](PF_6)_2$ formed in an 80% yield. M.p. 169–173 °C (dec). Anal. Calc for $C_{28}H_{36}N_8O_4F_{12}P_2Ag_2$: C 31.9; H 3.4; N 10.6. Found: C 31.9; H 3.4; N 10.7. IR (KBr pellets, cm^{-1}): 2964 (w), 2808 (m), 1720 (s), 1408 (m), 1286 (s), 1128 (s), 966 (m), 831 (s), 752 (m), 704 (m), 560 (m).

Synthesis of $[Ag_2(NO_3)_2(bip)]$

Colorless crystals of $[Ag_2(NO_3)_2(bip)]$ formed in a 75% yield. M.p. 172–176 °C (dec). Anal. Calc for $C_{20}H_{24}Ag_2N_6O_{10}$: C 33.1; H 3.3; N 11.6. Found: C 33.1; H 3.3; N 11.6. IR (KBr pellets, cm^{-1}): 2964 (w), 2945 (w), 2808 (w), 1722 (s), 1560 (m), 1365 (s), 1286 (s), 1128 (s), 949 (m), 756 (m), 706 (m), 692 (m).

Crystal structure determination

All X-ray data were collected on a Bruker SMART automatic diffractometer with graphite-monochromated Mo Kα radiation ($\lambda = 0.71073$ Å) and a CCD detector at 170 or

Table 1 Crystal and structure refinement data

Data	$[Ag_2(NO_3)_2(bip)]$	$[Ag_2(CF_3SO_3)_2(bip)(CH_3CN)_2]$	$[Ag_2(ClO_4)_2(bip)(CH_3CN)_2]$		$[Ag_2(BF_4)_2(bip)(CH_3CN)_2]$	$[Ag_2(bip)(CH_3CN)_4](PF_6)_2$
Empirical formula	$C_{20}H_{24}Ag_2N_6O_{10}$	$C_{13}H_{15}AgF_3N_3O_5S$	$C_{24}H_{30}Ag_2Cl_2N_6O_{12}$	$C_{24}H_{30}Ag_2Cl_2N_6O_{12}$	$C_{12}H_{15}AgBF_4N_3O_2$	$C_{14}H_{18}AgF_6N_4O_2P$
Formula weight	724.19	490.21	881.18	881.18	427.95	527.16
Temperature [K]	170(2)	170(2)	170(2)	298(2)	170(2)	170(2)
Crystal system	Monoclinic	Triclinic	Monoclinic	Monoclinic	Triclinic	Triclinic
Space group	$C2/c$	$P\bar{1}$	$P2_1/n$	$P2_1/n$	$P\bar{1}$	$P\bar{1}$
a [Å]	15.9415(2)	8.5428(1)	10.1934(2)	10.1663(2)	7.0589(2)	7.5885(1)
b [Å]	12.1518(2)	8.6000(1)	12.4329(2)	12.7630(2)	10.1784(2)	12.1154(2)
c (Å)	14.3405(3)	12.7017(1)	12.2365(2)	12.2723(2)	12.1987(3)	12.6257(2)
α [°]		76.693(1)			69.725(1)	115.122(1)
β [°]	119.7900(10)	75.684(1)	104.426(1)	104.777(1)	88.051(1)	104.551(1)
γ [°]		70.845(1)			73.299(1)	97.682(1)
Volume [$Å^3$]	2410.90(7)	842.73(2)	1501.88(5)	1539.70(5)	785.37(3)	978.26(3)
Z	4	2	2	2	2	2
D_{calc} [g/cm^3]	1.995	1.932	1.949	1.901	1.810	1.790
μ [mm^{-1}]	1.694	1.383	1.555	1.517	1.335	1.185
Max./min. transmission	0.8226/0.7070	0.7443/0.7202	0.9548/0.9249	0.7217/0.5485	0.6595/0.6039	0.5945/0.5516
hkl ranges	$-21 \le h \le 18$	$-11 \le h \le 11$	$-11 \le h \le 13$	$-13 \le h \le 13$	$-9 \le h \le 9$	$-8 \le h \le 10$
	$-16 \le k \le 13$	$-11 \le k \le 11$	$-16 \le k \le 16$	$-14 \le k \le 17$	$-13 \le k \le 13$	$-16 \le k \le 16$
	$-17 \le l \le 19$	$-16 \le l \le 16$	$-16 \le l \le 15$	$-16 \le l \le 16$	$-16 \le l \le 16$	$-16 \le l \le 16$
Total reflections	8822	15296	14736	15267	14157	17482
Unique reflections	2999	4148	3718	3838	3869	4784
R(int)	0.0175	0.0215	0.0247	0.0229	0.0199	0.0217
Parameters/restraints	172/0	236/0	194/0	209/0	209/0	239/0
R_1^a (all data)	0.0250	0.0233	0.0247	0.0332	0.0215	0.0400
R_1^a $I > 2\text{sigma}(I)$	0.0210	0.0212	0.0295	0.0415	0.0215	0.0376
wR_2^b (all data)	0.0533	0.0572	0.0577	0.0874	0.0659	0.1026
wR_2^b $I > 2\text{sigma}(I)$	0.0518	0.0503	0.0600	0.0922	0.0563	0.1003
Max./min. residual [$e/Å^{-3}$]	0.509/−0.309	0.404/−0.435	0.646/−0.427	0.711/−0.476	0.535/−0.488	1.365/−1.345
Goodness-of-fit on F^2	1.048	1.099	1.079	1.061	1.118	1.031

[a] $R_1 = \sum||F_o| - |F_c||/\sum|F_o|$

[b] $wR_2 = [\sum w(F_o^2 - F_c^2)^2/\sum wF_o^2]^{1/2}$

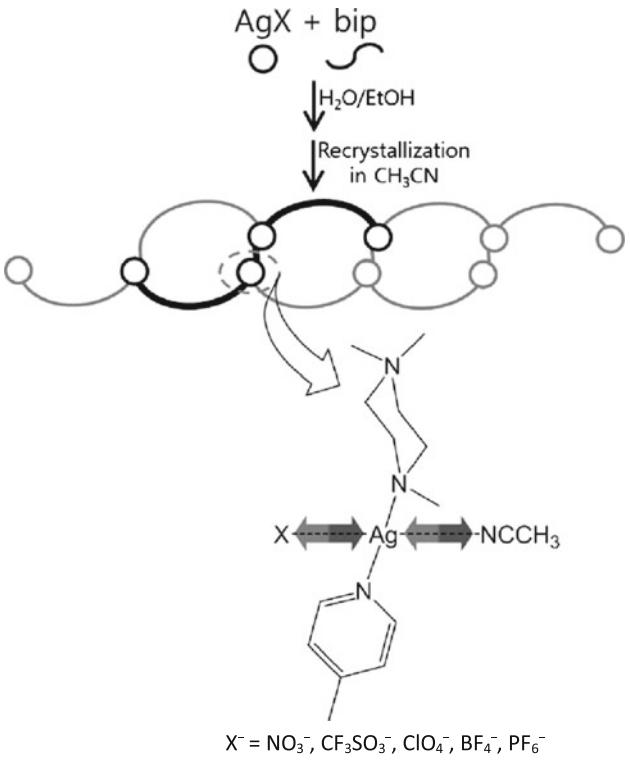

Scheme 1

298 K. Thirty-six frames of two dimensional diffraction images were collected and processed to obtain the cell parameters and orientation matrix. The data were corrected for Lorentz and polarization effects, and the absorption effects were corrected using the multi-scan method. The structures were resolved by the direct method (SHELXS 97) and refined using full-matrix least squares techniques (SHELXL 97) [27, 28]. The non-hydrogen atoms were refined anisotropically, and the hydrogen atoms were placed in calculated positions and refined using a riding model. The crystal parameters and procedural information corresponding to the data collection and structure refinement are listed in Table 1.

Results and discussion

Construction and crystal structures

The reaction of AgX ($X^- = NO_3^-$, $CF_3SO_3^-$, ClO_4^-, BF_4^-, and PF_6^-) with 1,4-bis(2-isonicotinoyloxyethyl)-piperazine (bip) in ethanol produced solid crude products (Scheme 1). These were recrystallized from acetonitrile to obtain single crystals of 2:1 (Ag/bip) complexes in high yields. All of the crystalline products are insoluble in water, chloroform, acetone, and alcohol, but soluble in acetonitrile, dimethyl sulfoxide, and *N,N*-dimethylformamide. The products were stable colorless solids for several days even in aqueous suspensions. The IR frequencies of the NO_3^-, $CF_3SO_3^-$, ClO_4^-, BF_4^-, and PF_6^- appeared at 1365, 1286, 1090, 1065, and 831 cm^{-1}, respectively (Supplementary material). The IR frequency of the ester moiety was in the 1720–1722 cm^{-1} range.

The asymmetric unit and extended structure of $[Ag_2(CF_3SO_3)_2(bip)(CH_3CN)_2]$ are shown in Fig. 1, and selected bond lengths and angles are listed in Table 2. The local geometry of the silver(I) atom is a four-coordinate arrangement with three nitrogen donors and one oxygen donor (Ag–N(pyridine), 2.152(1) Å; Ag–N(piperazine),

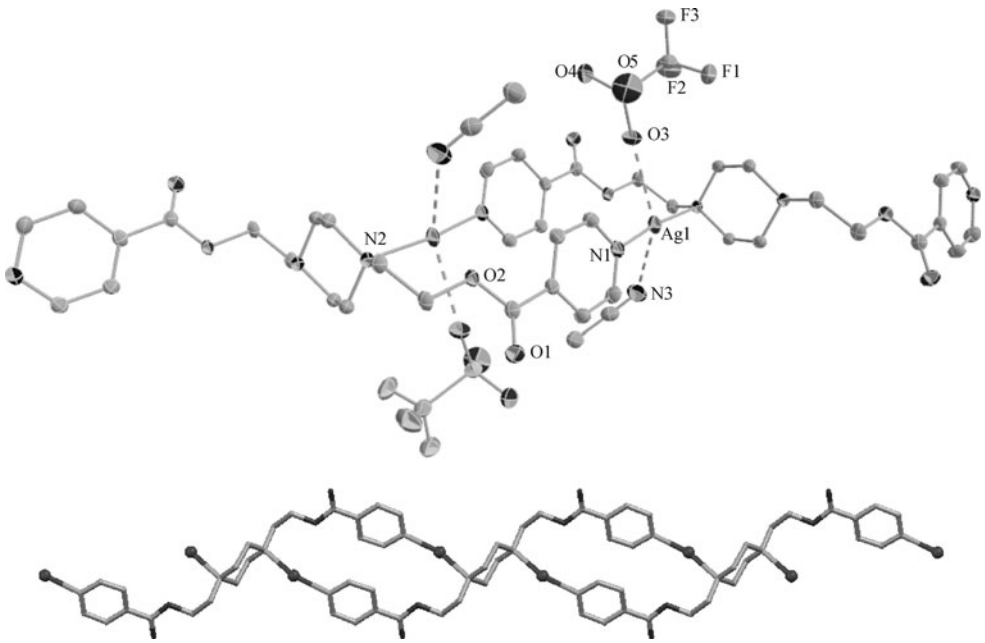

Fig. 1 X-ray structure of $[Ag_2(CF_3SO_3)_2(bip)(CH_3CN)_2]$ with thermal ellipsoids shown at 50% probability (*top*) and infinite structure (*bottom*). For clarity, the hydrogen atoms were omitted

Table 2 Selected bond distances [Å] and angles [°]

	$[Ag_2(NO_3)_2$ (bip)]	$[Ag_2(CF_3SO_3)_2$ (bip)$(CH_3CN)_2]$	$[Ag_2(ClO_4)_2$ (bip)$(CH_3CN)_2]$	$[Ag_2(BF_4)_2$ (bip)$(CH_3CN)_2]$	$[Ag_2$(bip) $(CH_3CN)_4](PF_6)_2$
Ag–X (Å)	2.554(2)	2.791(1)	2.821(3)	2.948(2)	4.055(7)
Ag–$NCCH_3$ (Å)		2.794(3)	2.691(2)	2.645(3)	2.672(4), 2.736(4)
Ag–N(pyridine) (Å)	2.206(2)	2.152(2)	2.230(2)	2.168(2)	2.198(2)
Ag–N(piperazine) (Å)	2.285(2)	2.230(1)	2.264(2)	2.242(2)	2.257(2)
N(1) Ag–N(2)′ (°)	151.52(6)	171.92(6)	159.62(6)	161.11(6)	169.17(9)

2.230(1) Å; Ag···N(acetonitrile), 2.794(3) Å; Ag···O, 2.791(1) Å). Each bip ligand acts as an N_4 tetradentate and is linked to the four silver(I) atoms through two pyridine and two piperazine moieties, producing a double strand consisting of two 20-membered ring units. The Ag(I)···$OSO_2CF_3^-$ (2.791(1) Å) distance is less than the sum of the van der Waals radii (3.20 Å) of Ag and O [29]. Interestingly, one acetonitrile molecule is coordinated with the silver(I) center as a third ligand, and one triflate acts as a fourth ligand. The packing structure is depicted in Fig. 2. The structures of $[Ag_2(ClO_4)_2(bip)(CH_3CN)_2]$ and $[Ag_2(BF_4)_2(bip)(CH_3CN)_2]$ are very similar to that of $[Ag_2(CF_3SO_3)_2(bip)(CH_3CN)_2]$ except for of the subtly different Ag···$NCCH_3$ and Ag···X lengths (Table 2 and Figs. 3, 4). Contrastingly, for $[Ag_2(NO_3)_2(bip)]$, the NO_3^- anion acts as a strong ligand (Ag···O = 2.554(2) Å) rather than a simple counteranion. The bond angle of N–Ag–N (151.52(6)°) is, concomitantly, bent. Thus, no acetonitrile is coordinated to the silver(I) center, resulting in tri-coordinate silver(I). For $[Ag_2(bip)(CH_3CN)_4](PF_6)_2$, two acetonitrile ligands are coordinated to one silver(I) center (Ag···N(acetonitrile) = 2.672(4), 2.736(4) Å) instead of the PF_6^- anion. The PF_6^- anion is a simple counteranion (the shortest Ag···F = 4.055(7) Å). For all products, Ag–N(py) is slightly stronger than Ag–N(piperazine).

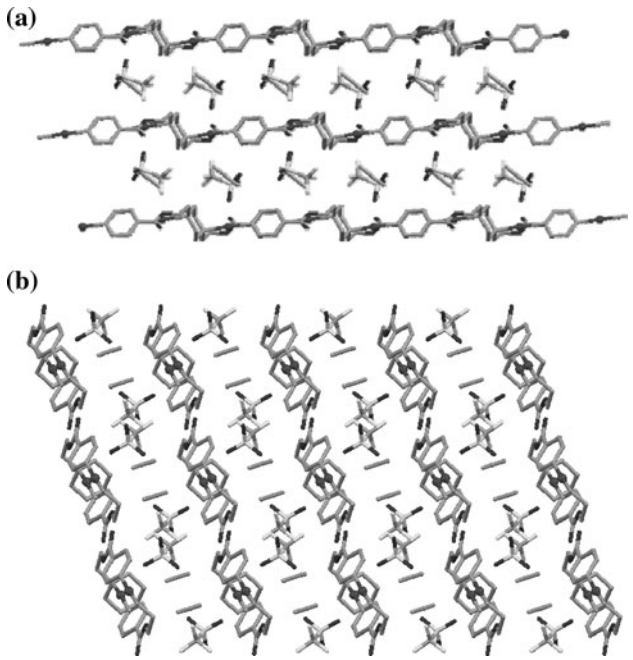

Fig. 2 Side view (**a**) and top view (**b**) of packing structure of $[Ag_2(CF_3SO_3)_2(bip)(CH_3CN)_2$

Polyatomic anion effects on construction

Our primary strategy was to appropriately combine silver(I) with a bidentate bip ligand. Unlike the case with the 1:1 cyclodimeric species [Ag(bpq)](BF$_4$) (bpq = 2,3-bis(pyridyl)quinoxaline) [30], the present reaction based on our design strategy resulted in the self-assembly of a 2:1 double strand Ag(I) : bip (Scheme 1). The skeletal double strand was efficiently constructed irrespective of the reactant stoichiometry and concentration. A key driving force of the construction is the potential tetradentate ligation of the bip ligand. The nature of an anion is significant to the coordination chemistry of the silver(I) center. For instance, the coordinating nature of NO_3^- is an obstacle to the coordination of acetonitrile. Weakly donating anions such as $CF_3SO_3^-$, ClO_4^-, and BF_4^- afford complexes with a single acetonitrile ligand. The PF_6^- anion, by contrast, induces two acetonitrile ligands. Thus, construction via coordination can be significantly affected by subtle anion differences. These facts are consistent with the Hoffmeister series [31]. A combination of a variety of geometries of silver(I) ions and the appropriate L ligand length, conformation, angle, and steric effects seems to afford characteristic structures of anion-dependent acetonitrile/silver(I) ratio. That is the acetonitrile/silver(I) ratio is strongly dependent on the nature of the anions. The PF_6^- anion, which has been considered as a common "non-coordinating" anion [32], has little tendency to serve as a ligand in the present structure. Such non-coordinating anions afford acetonitrile-abundant products. Alternatively, a relatively coordinating anion, NO_3^-, prevents acetonitrile coordination, resulting in a non-acetonitrile product,

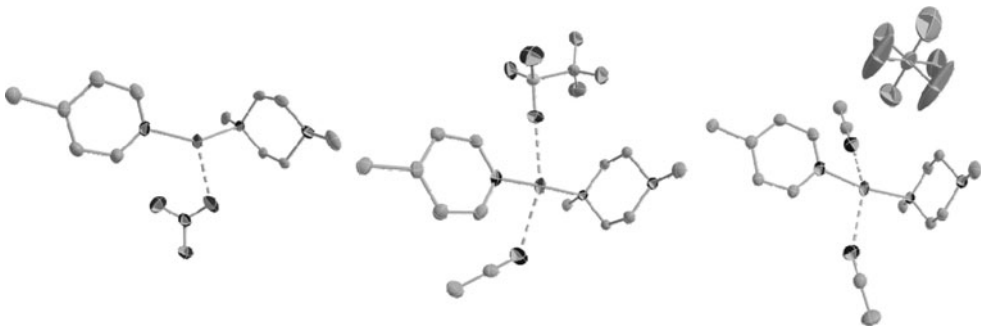

Fig. 3 Coordination environment of $[Ag_2(NO_3)_2(bip)]$ (*left*), $[Ag_2(CF_3SO_3)_2(bip)(CH_3CN)_2]$ (*middle*), and $[Ag_2(bip)(CH_3CN)_4](PF_6)_2$ (*right*). Those of $[Ag_2(ClO_4)_2(bip)(CH_3CN)_2]$ and $[Ag_2(BF_4)_2(bip)(CH_3CN)_2]$ are similar to that of $[Ag_2(CF_3SO_3)_2(bip)(CH_3CN)_2]$

$[Ag_2(NO_3)_2(bip)]$. A moderately coordinating anion, meanwhile, produces a single acetonitrile product. Acetonitrile/silver(I) ratios are exactly correlative with the order of the coordinating ability of polyatomic anions, reported in our previous paper [31]. Thus, the coordination as well as the local geometries of products appears to be subtly associated with the coordinating nature of the anions. The acetonitrile/silver(I) ratios increase with diminishing coordinating ability of the polyatomic anion ($NO_3^- \ll CF_3SO_3^- < ClO_4^- < BF_4^- \ll PF_6^-$), as shown in Fig. 4. Concomitantly, the ligand conformation in each complex seems to be dependent on the nature of the anions. Thus, a salient feature is that the coordinating ability of polyatomic anions is inversely proportional to that of acetonitrile.

Temperature effects

In order to clearly understand the temperature effects of coordination, the crystal structure of $[Ag_2(ClO_4)_2(bip)(CH_3CN)_2]$ was analyzed at both 170 and 298 K, and the results were compared. All of the crystallographic parameters, including the cell volume and density, showed significant 2% differences corresponding to the two temperatures (Table 1). As expected, for $Ag\cdots NCCH_3$ and $Ag\cdots OClO_3^-$, the distances (2.691; 2.821 Å) at low temperature were shorter than those (2.760; 2.832 Å) at high temperature. The difference in the $Ag\cdots NCCH_3$ length was the most significant. The Ag–N (Py, piperazine) lengths were relatively unaffected by the temperature change. Of course, the temperature effect was less significant than the anion effect.

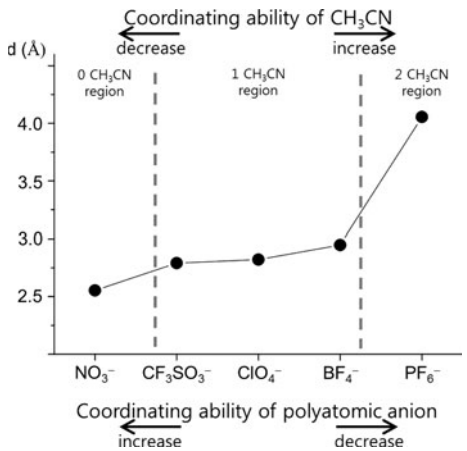

Fig. 4 Plot of Ag···X distances indicating relationship between Ag-$NCCH_3$ and Ag–X distances

Conclusions

The results of the present study are a good example of the fact that polyatomic anions are very competitive with acetonitrile in their ligation. Specifically, the acetonitrile/silver(I) ratio increases with decreasing coordinating ability. Our results also demonstrate that the present double strand skeleton is very stable against subtle changes in the nature of coordination. The construction and related properties of the molecular double strand could contribute to the construction and development of desirable molecular-based coordination materials.

Acknowledgment This work was supported financially by NRF-2008-313-C00426 in Korea.

References

1. Bradshow D, Claridge JB, Cussen EJ, Prior TJ, Rosseinsky MJ (2005) Acc Chem Res 38:273
2. Moulton B, Zaworotko MJ (2001) Chem Rev 101:1629
3. Constable EC (1992) Tetrahedron 48:10013
4. Jung OS, Kim YJ, Lee YA, Park JK, Chae HK (2000) J Am Chem Soc 122:9921
5. Jung OS, Kim YJ, Kim KM, Lee YA (2002) J Am Chem Soc 124:7906
6. Stang PJ, Olenyuk B (1997) Acc Chem Res 30:502
7. Albrecht M (1999) Angew Chem Int Ed 38:3463
8. Jones CJ (1998) Chem Soc Rev 27:289

9. Fujita M (1998) Chem Soc Rev 27:417
10. Batten SR, Robson R (1998) Angew Chem Int Ed 37:1460
11. Park BI, Chun IS, Lee YA, Park KM, Jung OS (2006) Inorg Chem 45:4310
12. Thanasekaran P, Liao TT, Liu YH, Rajendran T, Rajagopal S, Lu KL (2005) Coord Chem Rev 249:1085
13. Jung OS, Kim YJ, Lee YA, Kang SW, Choi SN (2004) Cryst Growth Des 4:23
14. Gale PA (2001) Coord Chem Rev 213:79
15. Beer PD, Smith DK (1997) Prog Inorg Chem 46:1
16. Jung OS, Kim YJ, Lee YA, Park KM, Lee SS (2003) Inorg Chem 42:844
17. Reed CA (1998) Acc Chem Res 31:133
18. Campos-Fernandez CS, Clerac R, Dunbar KR (1999) Angew Chem Int Ed 38:3477
19. Turner B, Shterenberg A, Kapon M, Suwinska K, Eichen Y (2001) Chem Commun 13
20. Sharma CVK, Griffin ST, Rogers RD (1998) Chem Commun 215
21. Withersby MA, Blake AJ, Champness NR, Hubberstey P, Li WS, Schröder M (1997) Angew Chem Int Ed Engl 36:2327
22. Wu HP, Janiak C, Rheinwald G, Lang H (1999) J Chem Soc Dalton Trans 183
23. Janiak C, Uehlin L, Wu HP, Klufers P, Piotrowski H, Scharmann TG (1999) J Chem Soc Dalton Trans 3121
24. Munakata M, Wu LP, Kuroda-Sowa T (1999) Adv Inorg Chem 46:173
25. Schmidtchen FP, Berger M (1997) Chem Rev 97:1609
26. Beer PD (1998) Acc Chem Res 31:71
27. Sheldrick GM (1997) SHELXS-97: a program for structure determination. University of Göttingen, Germany
28. Sheldrick GM (1997) SHELXL-97: a program for structure refinement. University of Göttingen, Germany
29. Huheey JE (1978) Inorganic chemistry, principles of structure and reactivity, 2nd edn. Harper & Row, New York
30. Jung OS, Park SH, Kim YJ, Lee YA, Jang HG, Lee U (2001) Inorg Chim Acta 312:93
31. Lee JW, Kim EA, Kim YJ, Lee YA, Pak Y, Jung OS (2005) Inorg Chem 44:3151
32. Chew KF, Healy MA, Khalil MI, Logan N, Derbyshire W (1975) J Chem Soc Dalton Trans 1315